

# Crystal structure, DNA binding studies, nucleolytic property and topoisomerase I inhibition of zinc complex with 1,10-phenanthroline and 3-methyl-picolinic acid

Hoi-Ling Seng · Sze-Tin Von · Kong-Wai Tan · Mohd Jamil Maah ·  
Seik-Weng Ng · Raja Noor Zaliha Raja Abd Rahman ·  
Igneiz Caracelli · Chew-Hee Ng

Received: 21 June 2009 / Accepted: 11 September 2009 / Published online: 29 September 2009  
© Springer Science+Business Media, LLC. 2009

**Abstract** Crystal structure analysis of the zinc complex establishes it as a distorted octahedral complex, *bis*(3-methylpicolinato- $\kappa^2N,O$ )<sub>2</sub>(1,10-phenanthroline- $\kappa^2N,N$ )-zinc(II) pentahydrate, [Zn(3-Me-pic)<sub>2</sub>(phen)]·5H<sub>2</sub>O. The *trans*-configuration of carbonyl oxygen atoms of the carboxylate moieties and orientation of the two planar picolinate ligands above and before the phen ligand plane seems to confer DNA sequence recognition to the complex. It cannot cleave DNA under hydrolytic condition but can slightly be activated by hydrogen peroxide or sodium ascorbate. Circular Dichroism and Fluorescence spectroscopic analysis of its interaction with various duplex polynucleotides reveals its binding mode as mainly intercalation. It shows distinct DNA sequence binding selectivity and the order of decreasing selectivity is

ATAT > AATT > CGCG. Docking studies lead to the same conclusion on this sequence selectivity. It binds strongly with G-quadruplex with human telomeric sequence 5'-AG<sub>3</sub>(T<sub>2</sub>AG<sub>3</sub>)<sub>3</sub>-3', can inhibit topoisomerase I efficiently and is cytotoxic against MCF-7 cell line.

**Keywords** Zinc(II) ternary complex · Duplex and quadruplex DNA binding · Nucleolytic · Topo I inhibition · Molecular modeling · Docking

## Introduction

Among the over 300 zinc metalloenzymes involve in cell functions and metabolism, zinc-finger topors have become prominent due their recently discovered role in tumour suppression (Stehbens 2003; Lin et al. 2005). Besides topoisomerase I, they can also bind to p53, AAV-2 Rep78/68 proteins and map to tumour suppressor genes on the human chromosome 9p21. Zinc-dependent endonucleases have been identified as one type of duplex DNA cleaving enzymes in plants (Jiang et al. 2008). Among enzymes which can cleave single stranded DNA are those which are zinc metalloenzymes or those which require zinc(II) for this property (Desai and Shankar 2003; Waterborg and Kuyper 1982). Consequently, the synthesis and

H.-L. Seng · S.-T. Von · C.-H. Ng (✉)  
Faculty of Engineering and Science, Universiti Tunku  
Abdul Rahman, 53300 Kuala Lumpur, Malaysia  
e-mail: ngch@utar.edu.my

K.-W. Tan · M. J. Maah · S.-W. Ng  
Chemistry Department, University of Malaya,  
50603 Kuala Lumpur, Malaysia

R. N. Z. R. A. Rahman  
Faculty of Biotechnology and Molecular Biology,  
Universiti Putra Malaysia, 43400 Serdang, Malaysia

I. Caracelli  
BioMat—Departamento de Física, Faculdade de Ciências,  
São Paulo State University, UNESP, Bauru 17015-970,  
Brazil

study of zinc(II) complexes have been regularly reported. An area of active research is the design and application of artificial, DNA-binding zinc finger proteins for recognition of diverse set of DNA sequences in a sequence-specific manner (Papworth et al. 2006; Nagaoka and Sugiura 2000). However, simple zinc(II) complexes with simple organic ligands having similar DNA sequence binding recognition are rare. Numerous zinc complexes are reported to be able to hydrolytically cleave DNA and RNA (Li et al. 2009; Bazzicalupi et al. 2008; Mancin and Tecilla 2007; Qian et al. 2007; Boseggia et al. 2004). However, some zinc complexes need activation by exogenous agent or a change in chemical environment or reaction condition for DNA cleavage (Ramakrishnan and Palaniandavar 2008; Seng et al. 2008).

DNA topoisomerases are important enzymes in the nucleus that modify the topological state of DNA through the introduction of transient breaks in the phosphodiester backbone of the DNA (Wang et al. 1998). They play essential roles in mitosis, particularly in DNA transcription and replication. These enzymes have been identified as important targets in cancer chemotherapy and microbial infections (Kumar Singh et al. 2007). In fact, topoisomerase I inhibitors are quoted as having a wide range of antitumor activities and are among the most widely used anticancer drugs clinically (Sunami et al. 2009; Rothenberg 1997; Beretta et al. 2008; Teicher 2008; Pommier 2008). However, not many metal complexes have been reported to inhibit topoisomerases. Very few zinc compounds have been reported to inhibit topoisomerase I and II (Kikuta et al. 2000; Chuang et al. 1996). A ternary zinc(II) complex of 1,10-phenanthroline and edda binds to duplex oligonucleotide ds(AT)<sub>6</sub> more selectively than ds(CG)<sub>6</sub>, and efficiently kills MCF-7 breast cancer cells by inducing cell cycle arrest (Ng et al. 2008).

Beside the above zinc ternary complex, other transition metal complexes are now being investigated as DNA binding agents and are now recognized to have both binding and DNA molecular recognition capabilities (Seng et al. 2008, 2009, unpublished data; Zeglis et al. 2007). Among them, octahedral metal complexes have been found to be able to differentiate different DNA conformations (B-, A- and Z-forms), to have binding site selectivity (minor or major groove; mismatched nucleobase sites) and to

have nucleobase sequence recognition (Zeglis et al. 2007). We are particularly interested in elucidating the nature of DNA molecular recognition of simple, varied geometrical metal complexes for different DNA structures and conformations, and nucleobase sequence recognition. For mononuclear metallointercalators, the intercalating ligand can anchor the metal complex between adjacent bases in differing intercalating mode and consequently orientate the other ligand(s) to interact with nucleobases in their vicinity. One particular aim of our work was to find out (1) whether both the main ligand and the auxiliary ligand(s) contribute to the DNA recognition and (2) type of interactive forces ( $\pi\cdots\pi$ , H-bonding, van der Waals, covalent) contributing towards the sequence recognition. Here, we report the crystal structure of a new zinc ternary complex, its nucleolytic property and its interaction with duplex DNA, various duplex oligonucleotides, G-quadruplex and topoisomerase I. Molecular modeling was carried out to further explore the binding selectivity among various duplex oligonucleotides.

## Materials and methods

### Materials

Most of the reagents were of analytical grade and were used as supplied. The pBR322, gene ruler 1 kb DNA ladder, 6× loading buffer, were bought from BioSyn Tech (Fermentas). Analytical grade agarose powder was purchased from Promega. CD<sub>3</sub>OD, Salmon testes DNA, calf-thymus DNA, sodium chloride (NaCl), human DNA topoisomerase I and ethidium bromide were purchased from Sigma Chemical Co. (USA). All solutions for DNA experiments were prepared with ultra-pure water from a Elga PURELAB ULTRA Bioscience water purification system with UV light accessory. The Tris–NaCl (TN) buffer was prepared from the combination of Tris base and NaCl dissolved in aqueous solution in which the pH was adjusted with hydrochloric acid (HCl) solution till pH 7.5. The Tris–NaCl buffer pH 7.5 contains Tris at 5 mM and NaCl at 50 mM unless otherwise stated. All stock solutions of H<sub>2</sub>O<sub>2</sub> and sodium ascorbate in deionized water and test compounds in Tris–NaCl buffer were freshly prepared daily.

## Methods

Elemental analysis of C, N and H was carried out on a Perkin Elmer 2400 CHN analyzer. The FTIR spectra of the complex were recorded as KBr disc in the range 4,000–400  $\text{cm}^{-1}$  on a Perkin Elmer FT-IR spectrometer.  $^1\text{H}$  NMR spectrum was recorded in deuterated methanol- $\text{D}_4$  on a JEOL ECA 400 MHz instrument. UV–visible spectroscopic measurement was carried out on a Perkin Elmer Lambda 40. Fluorescence measurements were performed using a Perkin-Elmer LS55 photoluminescence spectrometer. Circular Dichroism (CD) study of the interaction of zinc complex with CT-DNA or ds(oligonucleotide) or G-quadruplex was carried out with a 1.0 cm or 1.0 mm quartz cells, respectively, using a Jasco J-810 spectropolarimeter.

### Synthesis of *bis*(3-methyl-picolinato- $\kappa^2\text{N},\text{O}$ )(1,10-phenanthroline)zinc(II) tetrahydrate

Zinc acetate monohydrate (0.22 g, 1 mmol) and 1, 10-phenanthroline (0.20 g, 1 mmol) were heated in ethanol (20 ml) for 1 h followed by addition of 3-methylpicolinic acid (0.274 g, 2 mmol). The mixture was stirred for 24 h at room temperature. The white precipitate formed from slow evaporation of the solvent was filtered off, wash with cold water and chloroform. IR (KBr): 3,403, 1,622, 15,798, 1,518, 1,450, 1,424, 1,364, 1,277, 1,242, 1,200, 1,143, 1,143, 1,123, 1,104, 867, 849, 804, 727, 707, 679, 639, 575, 421  $\text{cm}^{-1}$ .  $^1\text{H}$  NMR( $\text{CD}_3\text{OD}$ ) (a) phen: 8.67 (d,  $J = 8$  Hz, 2H), 8.52 (s, 2H), 8.31 (s, 2H), 8.02 (s, 2H); (b) 3-methyl-picolinate: 7.92 (d,  $J = 8$  Hz, 2H), 7.87 (m,  $J = 8$  Hz, 2H), 7.52 (s, broad, 2H), 2.75 (s, 3- $\text{CH}_3$ , 6H). Anal. calcd. for  $\text{Zn}(\text{C}_{12}\text{H}_8\text{N}_2)(\text{C}_7\text{H}_6\text{NO}_2)_2 \cdot 4\text{H}_2\text{O}$ : C 52.94; H 4.78; N 9.50 found: C 53.28, H 4.61, N 10.05. Recrystallizing the white solid from water/methanol mixture (1:1) yielded crystals suitable for X-ray crystal structure analysis.

### Determination of crystal structure

The unit cell parameters and the intensity data were collected on a Bruker SMART APEX CCD diffractometer, equipped with a graphite monochromated  $\text{MoK}_\alpha$  X-ray source ( $\lambda = 0.71073$  Å). The APEX2 software was used for data acquisition and the SAINT

software for cell refinement and data reduction (Bruker 2007). Absorptions corrections on the data were made using SADABS (Sheldrick 1996). SHEL-XL97 was used for solving and refinement of the structure (Sheldrick 2008). The structure was solved by direct-methods and refined by a full-matrix least-squares procedure on  $F^2$  with anisotropic displacement parameters for non-hydrogen atoms. Hydrogen atoms in their calculated positions were refined using a riding model. The crystal data details are summarised in Table 1 while selected bond lengths and angles are given in Table 2.

### DNA cleavage experiments

Agarose gel electrophoresis experiments were carried out on supercoiled plasmid DNA pBR322 (4.4 kb) using a horizontal gel system. For the cleavage studies, each 20  $\mu\text{l}$  sample consisted of the complex dissolved in buffer, DNA, and the required volume of additional buffer. All samples were incubated in the dark in an incubator at a temperature of 37°C. The reaction mixtures were prepared as follows: 1  $\mu\text{l}$  of 50  $\mu\text{M}$  compound or salt were added to the mixture of 0.5  $\mu\text{l}$  of supercoiled plasmid DNA pBR322 (0.25  $\mu\text{g}/\mu\text{l}$ ) and Tris–NaCl buffer pH 7.5 was added to give a total volume of 20  $\mu\text{l}$ . The reactions were performed after incubating the reaction mixtures at 37°C for 24, 48 or 72 h. Three microliter of 6 $\times$  loading buffer was added to 20  $\mu\text{l}$  of the reaction mixtures and electrophoresis was performed at 80 V for 90 min in Tris–acetate-EDTA (TAE) buffer, pH 8.1, using 1.5% agarose gel. After electrophoresis, the agarose gel was stained with ethidium bromide solution (0.5  $\mu\text{g}/\text{ml}$ ). For the oxidative or reductive cleavage studies, incubation of the samples was similarly carried out. The DNA cleavage profile was analyzed using 1.5% agarose gel in a horizontal gel tank set with a running time of 2 h, at a constant voltage of 80 V. Each reaction mixture consisted of 0.5  $\mu\text{g}/\mu\text{l}$  DNA and Tris–NaCl buffer pH 7.5 unless otherwise mentioned. The resultant DNA bands after the electrophoresis step for each set of experiments were stained with ethidium bromide before being photographed under UV light using a Syngene Bio Imaging system and the digital image was viewed with Gene Flash software.

For the DNA cleavage by compound in the absence of exogenous agent, mechanistic experiments were

**Table 1** Crystal data and structure refinement of zinc(II) complex

CCDC deposition number	731838	$V$ (Å <sup>3</sup> )	2,708.67(12)
Chemical formula	C <sub>26</sub> H <sub>30</sub> N <sub>4</sub> O <sub>9</sub> Zn	$D$ (calc) (g cm <sup>-3</sup> )	1.491
Formula weight	607.91	$\mu$ (mm <sup>-1</sup> )	0.967
Crystal colour	Colourless	$F(000)$	1,264
Crystal size (mm)	0.100 × 0.150 × 0.200	$\theta_{\min/\max}$ (°)	1.76–27.50
$T(K)$	100(2)	Index ranges	$12 \leq h \leq 12, -21 \leq k \leq 23, -18 \leq l \leq 20$
Wavelength (Å)	0.71073	Reflections collected	6,163
Radiation	MoK $\alpha$	Independent reflections	4,324
Crystal system	Monoclinic	Refinement method	Full-matrix least-squares on $F^2$
Space group	P2 <sub>1</sub> /c	Data/restraints/parameters	6163/12/363
$Z$	4	Goodness-of-fit on $F^2$	1.031
$a$ (Å)	9.8979(2)	Final $R$ indices [ $I > 2\sigma(I)$ ]	$R_1 = 0.0507, wR_2 = 0.1325$
$b$ (Å)	18.3407(5)	$R$ indices (all data)	$R_1 = 0.0812, wR_2 = 0.1493$
$c$ (Å)	15.4779(4)	$\rho_{\min/\max}$ (e Å <sup>3</sup> )	0.749 and -0.805
$\alpha$ (°)	90.00		
$\beta$ (°)	105.417(2)		
$\gamma$	90.00		

**Table 2** Selected bond lengths and angles of zinc(II) complex

Bond lengths (Å)			
Zn1–O1	2.058(2)	C1–O1	1.273(4)
Zn1–O3	2.102(2)	C1–O2	1.242(4)
Zn1–N1	2.133(3)	C8–O3	1.263(4)
Zn1–N2	2.136(3)	C8–O4	1.220(4)
Zn1–N3	2.157(3)		
Zn1–N4	2.178(3)		
Bond angles (°)			
O1–Zn1–O3	166.62(9)	N2–Zn1–N3	94.68(11)
O1–Zn1–N1	77.49(10)	O1–Zn1–N4	100.78(10)
O3–Zn1–N1	92.41(10)	O3–Zn1–N4	88.53(9)
O1–Zn1–N2	95.06(10)	N1–Zn1–N4	94.03(10)
O3–Zn1–N2	77.11(10)	N2–Zn1–N4	162.74(10)
N1–Zn1–N2	96.08(11)	N3–Zn1–N4	77.12(10)
O1–Zn1–N3	95.50(10)	C1–O1–Zn1	117.8(2)
O3–Zn1–N3	95.93(10)	C8–O3–Zn1	117.4(2)
N1–Zn1–N3	167.63(10)		

similarly carried out to test the effect of radical scavengers, viz. sodium azide (NaN<sub>3</sub>), thiourea, and tiron, on the DNA cleavage was also used to test any cleavage inhibition. All final reaction mixtures were obtained by topping up with Tris–NaCl buffer pH 7.5.

## DNA binding studies

Stock solutions of calf thymus DNA (CT-DNA) was prepared by dissolving the DNA in buffer solution at 4°C, and the resultant homogeneous solutions were used within 2 days. The concentration of CT-DNA per nucleotide phosphate was calculated from the absorbance at 260 nm by using  $\epsilon = 6,400 \text{ M}^{-1} \text{ cm}^{-1}$ . The purity of the DNA was checked by monitoring the absorbance at 260 and 280 nm. PAGE grade self-complementary 12-mer oligonucleotides (CG)<sub>6</sub>, (AT)<sub>6</sub>, (CGCGAATTCGCG), (CGCGATATCGCG), HPLC grade G-quadruplex 22-mer oligonucleotide 5'-AGGGTTAGGGTTAGGGTTAGGG-3', and 17-mer complementary oligonucleotides 5'-CCAGTTCGTAGTAACCC-3', 3'-GGTCAAGCATCATTGGG-5' were annealed, to give the respective duplex, as specified by the supplier, 1st BASE and Eurogentec Ait. The circular dichroism spectra were obtained by scanning Tris–NaCl buffered solutions of the DNA without and with [Zn(3-methyl-pic)<sub>2</sub>(phen)]. Fluorescence (FL) emission spectra were recorded in the wavelength range 270–420 nm by exciting the respectively solutions with light at 226 nm. Excitation and emission slits were set at 10 nm. Solutions of DNA, and a series of [Zn(3-methyl-pic)<sub>2</sub>(phen)] was prepared in TN buffer (5 mM Tris, 50 mM NaCl) at pH 7.5 unless specifically stated. All the CD spectral bands

of the DNA alone and with the zinc complex are tabulated in Table 3.

### Ethidium bromide displacement assay

Ethidium bromide displacement assay were performed by measuring the emission of ethidium bromide bound to DNA which shows the enhanced emission intensity due to its intercalative binding to DNA. The competitive binding of the metal complex to the DNA reduces the emission intensity of ethidium bromide (EB) with either the bound complex quenching the emission or a displacement of the bound ethidium bromide from the bound to the free state. Fluorescence measurements were performed using a Perkin-Elmer LS55 photoluminescence spectrometer. All the fluorescence measurements were taken at  $\lambda_{\text{ex}}$  of 545 nm and  $\lambda_{\text{em}}$  of 600 nm at room temperature.

For determination of binding constant of zinc complex with CT-DNA, a TN buffer (5 mM Tris, 50 mM NaCl) at pH 7.5 was used. Prior to titration with the zinc complex, each 3 ml mixture of ethidium bromide, EB (0.32  $\mu\text{M}$ ) and CT-DNA (10  $\mu\text{M}$ ) is incubated for 24 h to allow saturation of DNA with EB. The detail of the procedure has previously been reported (Seng et al. 2009, unpublished data). For the corresponding determination of binding constant with

duplex deoxyoligonucleotides, the optimized conditions were based on previously reported procedure for high-throughput screening of DNA of short nucleotide sequences (Boger et al. 2001). The ratio of duplex:EB is 1:2 and the TN buffer (pH 7.5) composition is 100 mM Tris and 100 mM NaCl. Prior to titration with zinc complex, each 3 ml mixture of EB (2  $\mu\text{M}$ ) and duplex oligo (1  $\mu\text{M}$ ) was incubated for 24 h to attain saturation. For both cases, the serial titration was completed by adding 1  $\mu\text{l}$  of increasing concentration of zinc complex from appropriate stock solutions to the series of 3 ml EB-DNA mixtures until the quenching of DNA-bound EtBr fluorescence exceeds 50%. The final reaction mixtures were incubated for 2 h before measurement of their fluorescence intensity. The fluorescence intensities were plotted against the complex concentration to yield a curve that showed the relative extent of quenching of DNA-bound EB (data not shown). The values of the apparent binding constant,  $K_{\text{app}}$ , of the  $[\text{Zn}(\text{3-Me-pic})_2(\text{phen})]$  complex were calculated from the equation  $K_{\text{app,complex}}[\text{complex}] = K_{\text{app,EB}}[\text{EB}]$  where  $K_{\text{app,EB}}$  is the apparent binding constant of EB assumed to be  $10^7 \text{ M}^{-1}$ ,  $K_{\text{app,complex}}$  is the apparent binding constant of complex,  $[\text{EB}]$  is the concentration of EB used and  $[\text{complex}]$  is the concentration of the complex at 50% quenching (Rajendran and Nair

**Table 3** CD spectral bands of duplex oligos alone and with zinc complex (ZC): wavelength,  $\lambda$  (degree of ellipticity,  $\Phi$ )

	$\lambda/\text{nm}$ ( $\Phi/^\circ$ )	
	(–) band	(+) band
15 $\mu\text{M}$ ds(AT) <sub>6</sub>	252(–1.93)	272(2.19)
15 $\mu\text{M}$ ds(AT) <sub>6</sub> + 120 $\mu\text{M}$ ZC	252(–1.98)	277(4.67); 297(1.89)
15 $\mu\text{M}$ ds(CG) <sub>6</sub>	253(–6.18)	279(3.32)
15 $\mu\text{M}$ ds(CG) <sub>6</sub> + 120 $\mu\text{M}$ ZC	253(–5.97)	283(2.47)
10 $\mu\text{M}$ ds(CGCGAATTCGCG) <sub>2</sub>	252(–3.82)	280(2.75)
10 $\mu\text{M}$ ds(CGCGAATTCGCG) <sub>2</sub> + 120 $\mu\text{M}$ ZC	252(–3.54)	278(3.24); 298(1.18)
10 $\mu\text{M}$ ds(CGCGATATCGCG) <sub>2</sub>	253(–2.72)	277(1.90)
10 $\mu\text{M}$ ds(CGCGATATCGCG) <sub>2</sub> + 120 $\mu\text{M}$ ZC	250(–2.58)	279(3.27); 297(1.37)
20 $\mu\text{M}$ (5'-CCAGTTCGTAGTAGTAACCC-3') (3'-GGTCAAGCATCATCATTGGG-5')	249(–1.70)	279(5.71)
20 $\mu\text{M}$ (5'-CCAGTTCGTAGTAGTAACCC-3') (3'-GGTCAAGCATCATCATTGGG-5') + 120 $\mu\text{M}$ ZC	252(–3.13)	239(–0.91); 280(10.82)
20 $\mu\text{M}$ G-quadruplex	233(0.35); 267(–2.41)	246(2.21); 295(3.64)
20 $\mu\text{M}$ G-quadruplex + 60 $\mu\text{M}$ ZC	234(0.70); 262(–2.93)	246(1.94); 280(4.08); 296(5.26)
20 $\mu\text{M}$ G-quadruplex + 120 $\mu\text{M}$ ZC	228(0.53); 262(–3.40)	246(1.49); 279(5.67); 296(5.82)

2006). The binding and quenching constants are given in Table 4.

#### Human DNA topoisomerase I inhibition assay

The human DNA topoisomerase I inhibitory activity was determined by measuring the relaxation of supercoiled plasmid DNA pBR322. Each reaction mixture contained 10 mM Tris-HCl, pH 7.5, 100 mM NaCl, 1 mM Phenylmethylsulfonyl fluoride,  $\alpha$ -Toluenesulfonyl fluoride, PMSF, and 1 mM 2-mercaptoethanol, 0.25  $\mu$ g plasmid DNA pBR322, 1 unit of human DNA topoisomerase I, and the test compound or zinc complex at a specified concentration. Total volume of each reaction mixture was 20  $\mu$ l and these mixtures were prepared on ice. Upon enzyme addition, reaction mixtures were incubated at 37°C for 30 min. The reactions were terminated by the addition of 2  $\mu$ l of 10% SDS, and then followed by 3  $\mu$ l of dye solution comprising 0.02% bromophenol blue and 50% glycerol. SDS is required to denature topoisomerase I, preventing further functional enzymatic activity. The mixtures was applied

to 1.2% agarose gel and electrophoresed for 5 h at 33 V with running buffer of Tris-acetate EDTA, TAE. The gel was stained, destained, and photographed under UV light using a Syngene Bio Imaging system and the digital image was viewed with Gene Flash software.

Same protocol was applied in the Human DNA topoisomerase I inhibition condition study. The only variation is the sequence in adding the main components (human DNA topoisomerase I, plasmid DNA pBR322, and zinc complex). Two conditions were studied in this assay. In the first condition, human DNA topoisomerase I was incubated with zinc complex at 37°C for 30 min and then DNA was added and the reaction mixture was incubated for another 30 min at the same temperature. In the second condition, zinc complex and DNA were incubated for 30 min at 37°C first before the addition of topoisomerase I. Then, the resultant reaction mixture was incubated for another 30 min at the same temperature. This is a preliminary result of an investigation into the mode of action of zinc complex on the Human DNA topoisomerase I.

**Table 4** Binding and quenching constant of zinc complex with duplex oligonucleotides

Complex concentration ( $\mu$ M) at 50% quenching	Binding constant ( $M^{-1}$ )	Quenching constant
ds(AT) <sub>6</sub>		
927	$2.157 \times 10^4$	0.012
923	$2.166 \times 10^4$	0.012
928	$2.155 \times 10^4$	0.011
ds(CG) <sub>6</sub>		
1,112	$1.798 \times 10^4$	0.010
1,100	$1.818 \times 10^4$	0.010
1,112	$1.798 \times 10^4$	0.010
ds(CGCGAATTCGCG) <sub>2</sub>		
1,270	$1.574 \times 10^4$	0.007
1,270	$1.574 \times 10^4$	0.007
1,278	$1.564 \times 10^4$	0.007
ds(CGCGATATCGCG) <sub>2</sub>		
1,121	$1.784 \times 10^4$	0.009
1,126	$1.776 \times 10^4$	0.008
1,121	$1.784 \times 10^4$	0.009
CT-DNA		
603	$5.306 \times 10^3$	0.018
606	$5.280 \times 10^3$	0.018
606	$5.280 \times 10^3$	0.018

## Docking simulations

The 3-D structures of DNA used for the docking simulations were obtained from the PDB (<http://www.rcsb.org/pdb/home/home.do>) and PDBSum (<http://www.ebi.ac.uk/pdbsum/>) data banks, and are double helices associated with ligands. The specific DNA structures used in the calculations are summarized in Table 5. The DNA structures were chosen as to allow an evaluation of the binding preference for AT and CG sequences. The H atoms for each of 2da8 and 1g3x (Malinina et al. 2002) were added using the VegaZZ 2.0.8 programme (Pedretti et al. 2002, 2003, 2004), in all other cases H atoms were included in the deposited data.

Docking simulations were carried out using the 4.01 GOLD (Genetic Optimization for Ligand Docking) program (Jones et al. 1995, 1997), which is based on Genetic Algorithms. This method allows partial flexibility of the hydroxyl groups of the respective DNA molecule and full flexibility of the ligand. In order to evaluate the GOLD scoring function, all water molecules were removed from the DNA molecules. The two last columns of Table 5 list the atom used as centre of the calculations and the radius of the sphere searched, respectively. For 1g3x and 2rou, a smaller sequence was evaluated in order to obtain a better comparison with the experimental results, these are designated 1g3xM and 2rouM, respectively.

The function fitted was GoldScore:

$$\text{Fitness} = S(\text{hb\_ext}) + 1.3750 \times S(\text{vdw\_ext}) + S_{\text{int}}$$

where  $S(\text{hb\_ext})$  is the DNA-ligand hydrogen bond score,  $S(\text{vdw\_ext})$  is the DNA-ligand van der Waals score,  $S_{\text{int}}$  is the score from intramolecular ligand interactions.

## MTT assay

All tissue culture reagents were obtained from Sigma and Life Technologies Inc., Gaithersburg, MD. The oestrogen receptor positive human breast adenocarcinoma cell line MCF-7 cells were grown in RPMI 1640 supplemented with 10% FBS, 0.025 M Hepes, 0.024 M sodium bicarbonate, 50 units/ml penicillin G/streptomycin sulfate at 37°C in 5% CO<sub>2</sub>. MTT assay was used to test the cytotoxicity of zinc(II) complex which was incubated with cells for 72 h and it was carried out as previously described (Ng et al. 2008).

## Results and discussion

### Crystal structure of complex

Recrystallising the white product  $[\text{Zn}(\text{3-Me-pic})_2(\text{phen})] \cdot 4\text{H}_2\text{O}$  yielded the complex  $[\text{Zn}(\text{3-Me-pic})_2(\text{phen})] \cdot 5\text{H}_2\text{O}$  with formula  $\text{C}_{26}\text{H}_{30}\text{N}_4\text{O}_9\text{Zn}$ , which

**Table 5** Parameters for the docking studies

Binding site	PDB code*	Sequences	Centre of calculation sphere	Radius (Å)
TA	1g3x	(CGCGAATTCGCG) <sub>2</sub>	O2; T19	20
TA				
AT	2da8	(GATATC) <sub>2</sub>	O2; T3	20
TA				
TA	1g3xM	Modified: (GAATTC) <sub>2</sub>	O2; T19	20
TA				
GC	2rou	(ATCGCGCGGCATG)	O2; C21	20
CG		(TAGCGCGCCGTAC)		
GC	2rouM	Modified: (GCGCGG)	O2; C21	20
CG		(CGCGCC)		
GC	1y9h	(CCATGCTACC) <sub>2</sub>	O2; G16	20
CG				

\*1g3x (Malinina et al. 2002); 2da8 (Addess et al. 1993); 2rou (Wang et al. 2008); 1y9h (Zhang et al. 2005)



crystallizes as a colourless block crystal with a dimension of  $0.100 \times 0.150 \times 0.200$  mm with Monoclinic crystal system in space group  $P2_1/c$ , lattice parameters  $a = 9.8979(2)$  Å,  $b = 18.3407(5)$  Å,  $c = 15.4779(4)$  Å,  $\alpha = 90.00^\circ$ ,  $\beta = 105.417(2)^\circ$ ,  $\gamma = 90.00^\circ$ ,  $F(000) = 1264$ , GOF = 1.031,  $R_1 = 0.0507$ ,  $wR_2 = 0.1325$ ,  $Z = 4$ ,  $D_{\text{calc}} = 1.491$  g cm $^{-3}$ ,  $V = 2,708.67(12)$  Å $^3$ . The crystal structure is shown as an ORTEP plot (50% probability ellipsoids) in Fig. 1 (lattice water molecules are not shown). Each of the two bidentate 3-methylpicolinate ligand coordinates via its carboxylate oxygen atom and the adjacent pyridine nitrogen atom while the 1,10-phenanthroline binds via its two nitrogen atoms. The two picolinate ligands are positioned on the other side of the N–N atoms of the coordinated phen ligand and each picolinate moiety is orientated such that its plane is approximately directed along the Zn–N bond of the coordinated phen. As a result, the four ligating nitrogen atoms occupy the equatorial positions. The coordination geometry is a severely distorted octahedron. Consequently, the Zn–N bond length (mean value = 2.151 Å) is longer than the Zn–O bond length (mean value = 2.081 Å). In contrast, the corresponding Zn–N and Zn–O bond lengths of the Zn-picolinate moieties are reverse in *bis*(pyridine-2,6-carboxylato- $\kappa^3N,O,O'$ )zinc(II) trihydrate (Okabe and Oya 2000) and in *trans-diaquabis*(3-hydroxypicolinato- $\kappa^2N,O$ ) zinc(II) dihydrate (Di Marco et al. 2004), i.e., the Zn–N bonds are shorter than the Zn–O bonds in these complexes. The carboxylate oxygen and carbonyl atoms of the 3-methyl-picolinate ligands form hydrogen bonds with the lattice water molecules. So, the 3-methyl picolinate ligand in this zinc complex can act as a H-bond acceptor while interacting with DNA unlike the coordinated ethylenediamine-*N,N'*-diacetate (edda) in *M*(phen)(edda) which has both H-bond donor and acceptor sites (Ng et al. 2008).

### DNA binding study

The interaction of the  $[\text{Zn}(\text{3-Me-pic})_2(\text{phen})]$  with (1) duplex oligonucleotides of various specified nucleotide sequences, and (2) quadruplex DNA of the 23-mer oligonucleotide 5'-AG $_3$ (T $_2$ AG $_3$ ) $_3$ -3' and its corresponding duplex were investigated with CD and FL spectroscopy. CD spectroscopy is a useful technique in diagnosing changes in DNA morphology during drug–DNA interactions, as the band due to

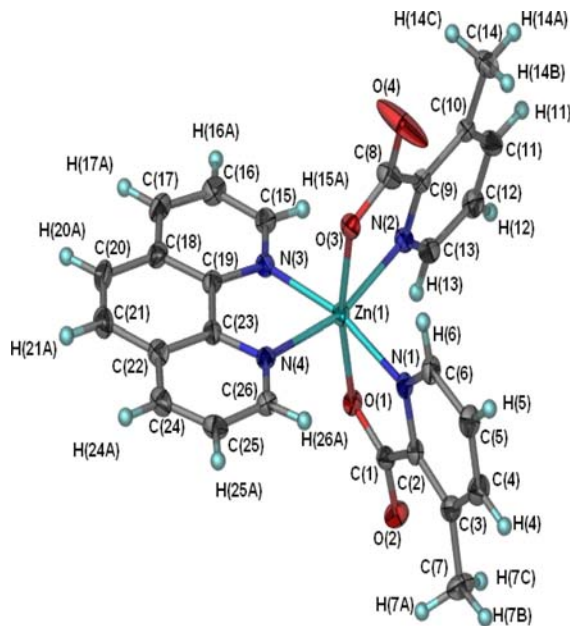


**Fig. 1** Ortep plot of *bis*(3-methylpyridine-2-carboxylato- $\kappa^2O,N$ )(1,10-phenanthroline- $\kappa^2N,N'$ )zinc(II) pentahydrate (50% probability ellipsoids). Water molecules are not shown

base stacking (275 nm) and that due to right-handed helicity (248 nm) are quite sensitive to the mode of DNA interactions with small molecules (Ivanow et al. 1973).

The CD spectra of all the duplex oligonucleotides show a negative band at  $\sim 250$  nm due to DNA helicity and a positive band at  $\sim 270$  nm due to base-pair stacking interaction, confirming the B-form conformation of these duplexes (Table 3). The first investigation was to find out any DNA binding preference for CG or AT sequences by the zinc complex. The zinc complex at a complex:duplex ratio of 1:8 greatly enhanced the positive band of the ds(AT) $_6$ , and this suggests the binding mode as intercalation (Fig. 2a; Seng et al. 2008). There is also a shift of the  $\lambda_{\text{max}}$  of the positive band from 272 to 277 nm and formation of an induced positive band at 297 nm. At the same mole ratio, the zinc complex does not induce a significant change in the CD spectrum of the ds(CG) $_6$ , suggesting binding with total retention of the B-form conformation (Fig. 2b). In terms of intensity enhancement  $\Delta\Phi$  at positive bands, the zinc complex induced a greater value (2.49 unit) for the ds(AT) $_6$  than that (0.85 unit) for the ds(CG) $_6$ . These results indicate stronger intercalation



**Fig. 2** **a** CD spectrum of 15  $\mu\text{M}$  of  $\text{ds(AT)}_6$  alone (I) and with 120  $\mu\text{M}$  of  $\text{Zn(phen)(3-methyl-pic)}_2$  (II) and **b** CD spectrum of 15  $\mu\text{M}$  of  $\text{ds(CG)}_6$  alone (III) and with 120  $\mu\text{M}$  of the zinc complex (IV)

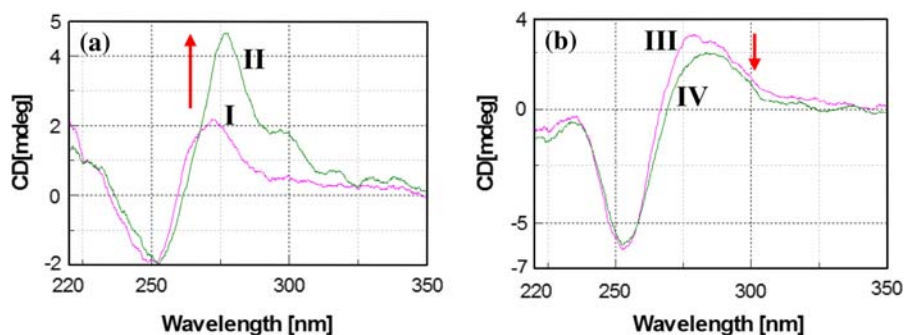
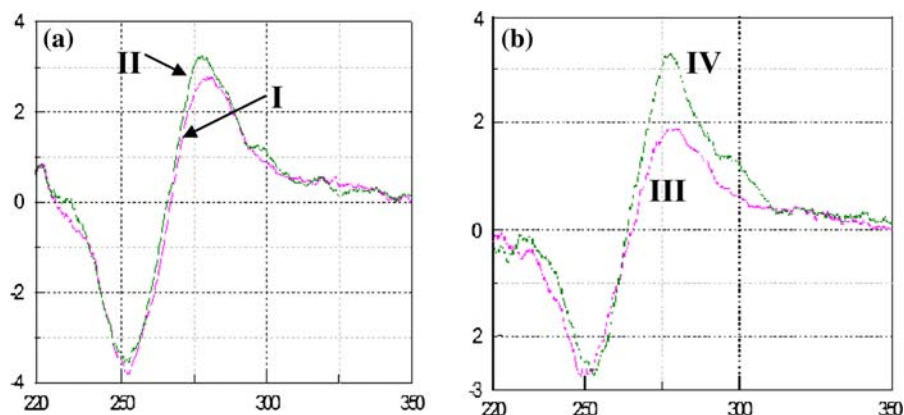


**Fig. 3** **a** CD spectrum of 10  $\mu\text{M}$  of  $\text{ds(CGCGAATTCGCG)}_2$  alone (I) and with 110  $\mu\text{M}$  of  $[\text{Zn(3-methyl-pic)}_2(\text{phen})]$  (II) and **b** CD spectrum of 10  $\mu\text{M}$  of  $\text{ds(CGCGATATCGCG)}_2$  alone (III) and with 110  $\mu\text{M}$  of the zinc complex (IV)



and binding selectivity of the zinc complex for the AT sequences. Similar results have been obtained for the (ethylenediamine- $N,N'$ -dicarboxylato- $\kappa^4N,N',O,O'$ ) (1,10-phenanthroline- $\kappa^2N,N'$ )zinc(II),  $\text{Zn(phen)(edda)}$  (Seng et al. 2008). Similar preferential binding to AT-rich DNA is also shown by one of the optical enantiomers of octahedral Ru(II) mononuclear or dinuclear polypyridine complexes (Nordell et al. 2007). The following enantiomers bind more selectively to AT-sites:  $\Lambda$ - $[\text{Ru(phen)}_3]^{2+}$ ,  $\Delta$ - $[\text{Ru(phen)}_2\text{dppz}]^{2+}$ , and  $\Delta\Delta$ -P (where P is a dimmer of  $[\text{Ru(phen)}_2\text{dppz}]^{2+}$  joined by a single bond). Zinc(II)-cyclen and zinc(II)-derivatized cyclen complexes (cyclen = 1,4,7,10-tetraazacyclododecane) were found to selectively bind to thymidine (dT) and uridine (U) in nucleosides and polynucleotides (Kikuta et al. 2000). Interestingly, the zinc(II) complexes of cyclen derivatives appended with one or two alkyl or aryl groups have been proven to selectively bind to an AT-rich TATA box of the promoter region of SV40 early gene.

We next investigated the interaction with  $\text{ds(CGCGAATTCGCG)}_2$  and  $\text{ds(CGCGATATCGCG)}_2$  oligonucleotides. For the first duplex, there is not much

change in CD spectrum due to binding of the zinc complex except for a slight enhancement of the positive band at  $\sim 278$  nm and a small induced band at 300 nm (Fig. 3a). The zinc complex induced a greater enhancement of the positive band (at  $\sim 277$  nm) of the CD spectrum of the  $\text{ds(CGCGATATCGCG)}_2$  at the same complex: duplex mole ratio (1:8) and a broadening of the negative band (Fig. 3b). As for the  $\text{ds(AT)}_6$  duplex, the zinc complex has induced a new positive band for the  $\text{ds(CGCGATATCGCG)}_2$  at 297 nm. Comparing the CD results of these four  $\text{ds(oligos)}_2$ , we infer that the chelated 1,10-phenanthroline of the zinc complex binds more selectively to ATAT sequence than to AATT sequence, and the resultant binding mode involving this ligand is intercalative. At the moment, we are unsure of the cause of the induced positive bands at  $\sim 300$  nm.

To investigate further the above nucleobase sequence selectivity, we used a EB displacement assay to obtain the apparent binding and quenching constants of the zinc complex with the four duplex oligonucleotides (Table 4). The apparent binding constants of the zinc complex for the  $\text{ds(AT)}_6$  and  $\text{ds(CG)}_6$  are

$2.159 \times 10^4$  and  $1.805 \times 10^4 \text{ M}^{-1}$ , respectively. Thus, the complex binds more strongly with  $\text{ds(AT)}_6$  and this correlates with greater enhancement of the positive band of the CD spectrum of  $\text{ds(AT)}_6$  compared to that with the  $\text{ds(CG)}_6$ . Similarly, the binding constants of the zinc complex for the  $\text{ds(CGCGA TATCGCG)}_2$  and  $\text{ds(CGCGAATTCGCG)}_2$  are  $1.781 \times 10^4$  and  $1.571 \times 10^4 \text{ M}^{-1}$ , respectively. The results of this assay is in agreement with the CD results, i.e., both data support the conclusion that the zinc complex has DNA binding selectivity for AT-repeat and ATAT sequences.

The AT selectivity observed for the neutral  $[\text{Zn(3-Me-pic)}_2(\text{phen})]$  complex may be different from that of cationic, square pyramidal  $[\text{Cu(phen)(L-arg)Cl}]^+$  which has higher binding constant  $K_{\text{app}}$  ( $1.11 \times 10^6 \text{ M}^{-1}$ ) for  $\text{poly(dA)·poly(dT)}$  than that ( $4.9 \times 10^5 \text{ M}^{-1}$ ) for  $\text{poly(dC)·poly(dG)}$  obtained from EB displacement assay (Patra et al. 2007). Computer simulation study of this copper complex using  $\text{ds(CGCGAATTCGCG)}_2$  shows favourable stacking interaction by the phen moiety and H-bonding interactions with the AT base pair sequences of this duplex and the positively charged guanidinium end group. However, an optically active ternary octahedral ruthenium complex,  $\Delta\text{-cis-}\alpha\text{-[Ru(RR-pic-chxnMe}_2\text{)(phen)]}^{2+}$  ( $\text{picchxnMe}_2 = N,N'\text{-dimethyl-}N,N'\text{-di(2-picolyl)-1,2-diaminocyclohexane}$ ), was shown via NMR study to bind with AT selectivity in the minor groove of  $\text{d(CGCGATCGCG)}_2$  and  $\text{d(ATATCGA TAT)}_2$  duplexes without intercalation of the phen ligand (Proudfoot et al. 1997). On the other hand, recognition of zinc(II)-cyclen derivatives for AT-rich regions involve the zinc atom covalently bonding to N(3)-deprotonated anionic form of the thymine and the stacking interaction of the aromatic substituent group(s) at the cyclen with aromatic ring of proximal nucleobase (Kikuta et al. 2000). Distamycin, a clinically useful non-metal drug, apparently recognise AT-rich regions of DNA mainly by hydrogen bonding to adenine N(3) and thymine O(2) (Kikuta et al. 2000; and references quoted therein). It is not self evident how these diverse set of compounds exhibit AT-selectivity and the factors responsible for such recognition or the basis of such recognition have not been properly analyzed and compared. However, the DNA binding selectivity of  $[\text{Zn(3-Me-pic)}_2(\text{phen})]$  may account for

the much lower binding constant of this complex for CT-DNA which has 50% CG and 50% AT (Table 4).

## Docking

To explore further the nature of the DNA binding selectivity by the  $[\text{Zn(3-Me-pic)}_2(\text{phen})]$ , a molecular modelling study using the Gold Program was undertaken. The chosen duplexes were (1) AT-rich duplexes  $\text{ds(GATATC)}_2$  (2da8) and  $\text{d(GAATTC)}_2$  (1g3xM), and (2) GC-rich duplexes  $\text{ds(CCATGC TACC)(GGTAGCGATGA)}$  (1y9h) and  $\text{ds(GCGC GC)(CGCGCG)}$  (2rouM) for docking simulation with the zinc complex (Table 5). The aim was to study the nucleobase sequence selectivity by computer simulation. The relative orientation and the interaction determined from the results of the docking study were analyzed using the graphical program: Discovery Studio Visualizer 2.0. The views in Fig. 4 show the different modes how the “ligand”  $[\text{Zn(3-Me-pic)}_2(\text{phen})]$  intercalated in the different DNA sequences. The different number of observed stacking  $\pi\cdots\pi$ , H-bonding,  $\text{C-H}\cdots\pi$  and  $\text{C=O}\cdots\pi$  interactions suggests that they are related to the strength of the ligand binding mode and is in accord with the obtained scores. The decreasing order of the scores for the duplexes with binding energy  $E$  (kcal/mol) is  $2\text{da8} (-70.38) > 1\text{g3xM} (-68.77) > 1\text{y9h} (-57.16) > 2\text{rou} (-54.62)$  (Table 6). An analysis of the interactions and the results of the score (Fig. 5; Tables 6, 7) suggest the order of nucleotide sequence binding selectivity as  $\text{ATAT} > \text{AATT} > \text{GC}$ . This order is in accord with the results of the earlier CD and FL binding studies.

Thus, the docking results are reliable and warrant further analysis and discussion of the nature of the sequence recognition. Preliminary assessment leads us to believe (1) that both the intercalating ligand (phen) and 3-methyl-picolinate ligands with only H-bonding acceptor atoms (Fig. 1: O1, O3, N1, N2) contribute to this recognition, and (2) that the orientations of the two 3-methyl-picolinate ligands with respect to the planar phen ligand is important. Intercalation of phen in a given site and mode anchor it to the DNA and direct the orientation of the two 3-Me-pic ligands for interaction with nucleobases in their vicinity. Here, we focus on the contribution from intercalation of the phen.

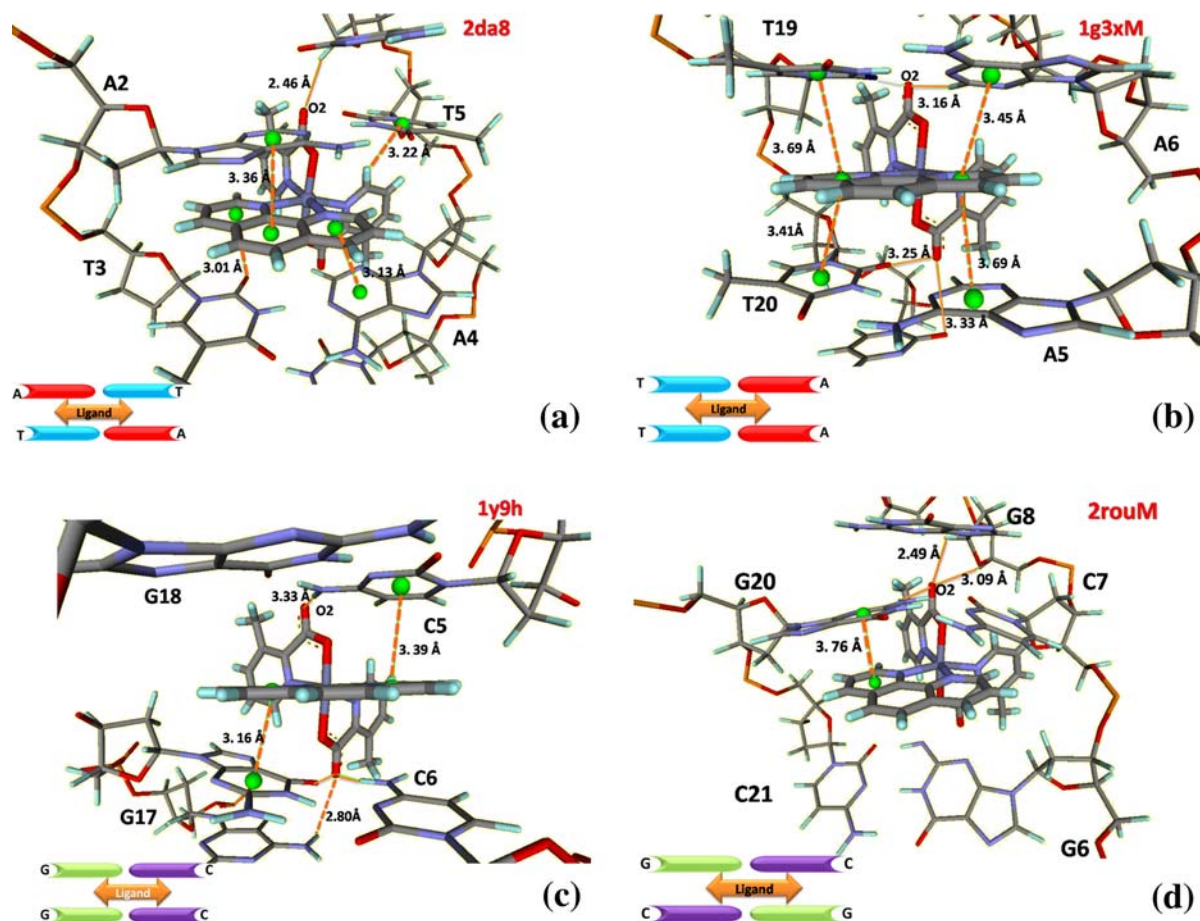


**Fig. 4** Views of the intercalation of [Zn(3-Me-pic)<sub>2</sub>(phen)] in the DNA molecules studied herein. In all diagrams the O2 atom of the ligand is positioned upwards. **a** 2da8 (ATAT) where four interactions involving  $\pi$  systems are seen: three rings of the ligand form  $\pi\cdots\pi$  interactions with the bases A2, A4 and T3, and a C–H $\cdots\pi$  interaction is also formed between the ligand

and the T5 base. **b** 1g3xM (AATT): two rings of the central part of the ligand interact with four bases (A5, A6, T19 and T20). **c** 1y9h (GGCC) two rings of the central part of the ligand form  $\pi\cdots\pi$  interactions with the C5 and G17 bases. **d** 2rouM, where the ligand is found to be the most weakly attached of the series, shows only one  $\pi\cdots\pi$  interaction, with the G20 base

(1) 2da8 = ds(GATATC)<sub>2</sub>

Binding energy,  $E = -70.3$  kcal/mol

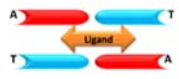



Phen moiety intercalates between A2/A4 diagonal base steps of different DNA strands, with central phen aromatic ring-nucleobase contact of 3.36 Å and adjacent phen aromatic ring-nucleobase contact distance of 3.13 Å, i.e., there are two  $\pi$ – $\pi$ , aromatic ring-aromatic ring interaction (i.e., stacking interaction). In contrast, the phen moiety of [Zn(phen)(edda)] intercalate between the A/A adjacent base steps of the same DNA strand (Seng et al. 2008).

(2) 1g3xM = ds(GAATTC)<sub>2</sub>

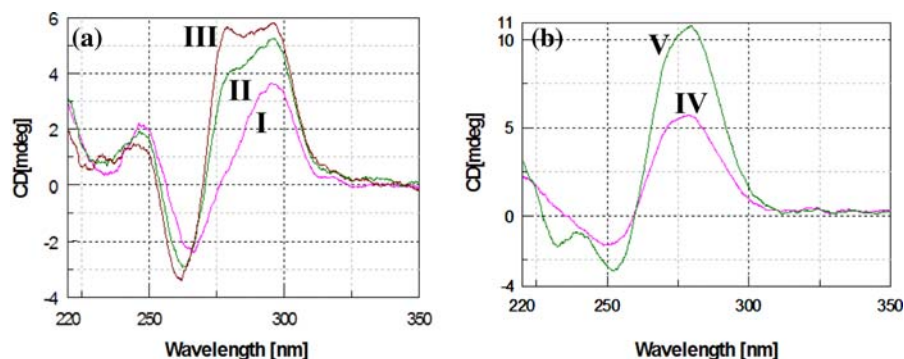
Binding energy,  $E = -68.77$  kcal/mol

Phen moiety intercalates between T19…A6/T20…A5 base-pairs, with each of the two side aromatic rings of the phen ligand making  $\pi$ – $\pi$  stacking interaction with base-pair above and that below the phen. The centroid–centroid distances for the T19-phen-T20 stacking interaction are 3.69 and 3.41 Å, respectively (Fig. 4b) and those for the A6-phen-A5 stacking interaction are 3.45 and 3.69 Å, respectively. These four  $\pi$ – $\pi$ , aromatic ring-aromatic ring interactions are weaker than

**Table 6** The scores for binding of zinc complex to various duplex oligonucleotides using docking calculations

binding site	PDB code	sequences	E (kcal/mol)	
	AT	2da8	(GATATC) <sub>2</sub>	-70.38
	TA	1g3xM	modified: (GAATTC) <sub>2</sub>	-68.77
	CG	1y9h	(CCATGCTACC) <sub>2</sub>	-57.16
	GC	2rouM	modified: (GCGCGG) (GCGGCC)	-54.62

**Fig. 5** **a** CD spectrum of 20  $\mu$ M of G-quadruplex 5'-AG<sub>3</sub>(T<sub>2</sub>AG<sub>3</sub>)<sub>3</sub>-3' alone (I) and with 60  $\mu$ M (II) and 120  $\mu$ M (III) of [Zn (3-methyl-pic)<sub>2</sub>(phen)] and **b** CD spectrum of 20  $\mu$ M of G-sequence duplex oligo alone (IV) and with 120  $\mu$ M of the zinc complex (V)



those for the zinc complex interaction with ds(GATATC)<sub>2</sub>.

(3) 1y9h = (CCATGCTACC)(GGTAGCGATGA)

Binding energy, E = −57.16 kcal/mol

Phen moiety intercalates between G17/C5 diagonal base steps of different DNA strands, with central phen aromatic ring-nucleobase contact of 3.16 Å and adjacent phen aromatic ring-nucleobase contact distance of 3.39 Å. These two  $\pi$ - $\pi$ , aromatic ring-aromatic ring interactions are comparative strong, compared to those found for the interaction of zinc complex with ds(GATATC)<sub>2</sub>.

(4) 2rouM = (GCGCGC)(GCGCGC)

Binding energy, E = −54.62 kcal/mol

Here, there is only one weak  $\pi$ - $\pi$ , aromatic ring-aromatic ring interaction between the phen moiety

and G20, with the centroid-centroid distance between phen-G20 of 3.76 Å.

From the above comparison of  $\pi$ - $\pi$  interactions and analysis of other types of interaction between the zinc complex and the respective duplexes, the higher selectivity of the zinc complex for the ATAT sequence of 2da8 duplex can be ascribed to the greater number of the types of interaction (Table 7) and their combined total binding energy, E (Table 6). The 2da8 has multiple H-bonding, involving nucleobases A2, T5, A4 and C6, with the zinc complex and has  $\pi$ ... $\pi$  (nucleobase...phen),  $\pi$ ... $\pi$  (thymine C=O...phen) and C-H... $\pi$  (picolinate...T5). All these contribute to making the zinc complex having the highest binding energy for 2da8. Thus, it seems reasonable to ascribe the recognition of the ATAT sequence by the zinc complex to these interactions. In contrast, the DNA recognition of zinc(II)-cyclen

**Table 7** Interactions between the DNA and Zn(3-Me-pic)<sub>2</sub>(phen)M ligand

2da8 Atom	Zn(3-Me-pic) <sub>2</sub> (phen)M atom	Distance (Å)
A2:H2	O2	2.691
T5:O2	H13	2.964
T5:H1 <sup>b</sup>	O2	3.247
A4:H2	O4	2.889
C6:H1 <sup>b</sup>	O2	2.463
T3:O2	Ct (C22–C23–N4–C26–C25–C24)	3.008
A2:Ct (N1–C2–N3–C4–C5–C6)	Ct (C18–C19–C20–C21–C22–C23)	3.359
A4:Ct (N1–C2–N3–C4–C5–C6)	Ct (N3–C15–C16–C17–C18–C19)	3.262
T5:Ct (N1–C2–N3–C4–C5–C6)	H13–C13	3.220
1g3xM atom	Zn(3-Me-pic) <sub>2</sub> (phen)M	Distance (Å)
T20:O4 <sup>a</sup>	H6	2.955
T20:O4 <sup>a</sup>	H25A	2.906
T20:O4 <sup>a</sup>	H26A	2.026
T20:O3 <sup>a</sup>	H5	3.271
T20:O2	O4	3.252
T20:H1 <sup>a</sup>	O4	3.351
C21:O2	O4	3.325
C21:H5 <sup>a</sup> 1	O4	3.396
T19:O2	O2	2.511
T19:H1 <sup>a</sup>	O2	3.317
A6:H2	O2	3.159
A5:Ct (N1–C2–N3–C4–C5–C6)	Ct (N3–C15–C16–C17–C18–C19)	3.693
A6:Ct (N1–C2–N3–C4–C5–C6)	Ct (N3–C15–C16–C17–C18–C19)	3.453
T19:Ct (N1–C2–N3–C4–C5–C6)	Ct (C22–C23–N4–C26–C25–C24)	3.694
T20:Ct (N1–C2–N3–C4–C5–C6)	Ct (C22–C23–N4–C26–C25–C24)	3.415
1y9h atom	Zn(3-Me-pic) <sub>2</sub> (phen)M atom	Distance (Å)
C7:H41	O4	3.243
G16:O6	O4	2.648
C5:Ct (N1–C2–N3–C4–C5–C6)	Ct (N3–C15–C16–C17–C18–C19)	3.393
G16:Ct (N1–C2–N3–C4–C5–C6)	Ct (C22–C23–N4–C26–C25–C24)	3.160
2rouM atom	Zn(3-Me-pic) <sub>2</sub> (phen)M atom	Distance (Å)
G8:H4 <sup>b</sup>	O2	3.088
G8:H1 <sup>b</sup>	O2	2.488
G9:H5 <sup>b</sup>	O2	3.164
G20:H21	O2	2.852
G20:H22	O2	2.371
C7:O4 <sup>b</sup>	H13	2.658
C7:O4 <sup>b</sup>	H15A	2.180
C7:O4 <sup>b</sup>	H16A	3.377
G20:Ct (N1–C2–N3–C4–C5–C6)	Ct (C22–C23–N4–C26–C25–C24)	3.763

Ct, centroid

<sup>a</sup> Atom of nucleobase thymine T19 or T20

<sup>b</sup> Atom of nucleobases cystine C7 or guanine G8



derivatives seems to be that it selectively binds to thymine by covalent bonding (Kikuta et al. 2000). In optically-active ruthenium complexes, chirality seems to confer only one of the enantiomers with binding selectivity for AT-sequences, e.g., both  $\Delta$ -[Ru(phen)<sub>2</sub>dppz]<sup>2+</sup> and  $\square$ -[Ru(phen)<sub>3</sub>]<sup>2+</sup> prefer AT-binding sites than GC- or mixed-sequence binding sites (Nordell et al. 2007). Some [Ru(Hdpa)<sub>2</sub>(diimine)](ClO<sub>4</sub>)<sub>2</sub> (Hdpa = 2,2'-dipyridylamine; diimine = 1,10-phenanthroline derivatives) complexes shows preferential binding to AT than to GC or mixed sequences but the origin of this selectivity was not explained (Rajendiran et al. 2008). Copper(II) bis-arginate [Cu(L-arg)<sub>2</sub>](NO<sub>3</sub>)<sub>2</sub> and [Cu(L-arg)(-phen)Cl]Cl as mimics of the minor-groove-binding natural antibiotic netropsin show preferential binding to the AT-rich region of double stranded DNA (Patra et al. 2007). It seems that the matching of the crescent shape of the copper complexes to the DNA minor groove, electrostatic interaction, multiple H-bonding between the positively charged guanidinium end group of L-arginate ligand with A and T bases, and stacking interaction of the phen ligand are contributing factors towards AT-recognition.

### G-quadruplex

Next, we use CD spectroscopy to investigate the interaction of the zinc complex with the single strand G-quadruplex DNA annealed from 5'-AG<sub>3</sub>(T<sub>2</sub>AG<sub>3</sub>)<sub>3</sub>-3' and with the duplex DNA annealed from two complementary 17 nucleotide primers, 5'-CCA GTTCGTAGTAACCC-3' and 3'-GGTCAAGCATC ATTGGG-5'. Single strand quadruplexes can assume parallel structure, antiparallel structure or a mixture of both (Kypr et al. 2009; Zhang et al. 2007; Baker et al. 2006). The CD spectrum of our G-quadruplex alone shows two maxima at 295 nm (degree of ellipticity,  $\Phi$  = 3.64 units) and 246 nm ( $\Phi$  = 2.20 arbitrary units), and a minimum at 267 nm ( $\Phi$  = -2.41 units) (Fig. 5, spectrum I). This spectrum is typical of other reported anti-parallel quadruplexes, viz. d(T<sub>2</sub>AG<sub>3</sub>)<sub>4</sub>, d(T<sub>2</sub>AG<sub>3</sub>)<sub>6</sub> and dAG<sub>3</sub>(T<sub>2</sub>AG<sub>3</sub>)<sub>3</sub> (Baker et al. 2006; Galezowska et al. 2007). Single strand, antiparallel G-quadruplexes can have two different strand orientations, viz. chair and basket (Baker et al. 2006). Oligonucleotides with human telomeric sequence, in the presence of Na<sup>+</sup> ion, form G-quadruplexes with antiparallel-stranded structures

with their guanines having alternating syn-anti glycosidic conformations and give a characteristic positive peak at 295 nm and two small peaks: a negative at 265 nm and a positive at 240 nm (Galezowska et al. 2007). CD data shows human telomeric sequence d[G<sub>3</sub>(T<sub>2</sub>AG<sub>3</sub>)<sub>3</sub>] formed antiparallel quadruplex in the presence of Na<sup>+</sup> but formed a hybrid mixture of parallel and antiparallel structures in the presence of K<sup>+</sup> (Lu et al. 2008). Based on CD data, this hybrid mixture was shown to be converted to wholly antiparallel structure by the addition of a 5-methylated quinoline derivative, *N'*-(5-*N*-Methyl-10*H*-indolo[3,2-*b*]quinolin-5-ium)-*N,N*-dimethyl-propane-1,3-diamine iodide. A previously reported human telomeric sequence d[AG<sub>3</sub>(T<sub>2</sub>AG<sub>3</sub>)<sub>3</sub>] in the presence of 100 mM Na<sup>+</sup> ions forms an antiparallel G-quadruplex structure, as evidenced (1) by its CD having a 295 nm positive band and 265 nm negative band and (2) by NMR studies (Xu et al. 2006). Thus, our G-quadruplex annealed from 5'-AG<sub>3</sub>(T<sub>2</sub>AG<sub>3</sub>)<sub>3</sub>-3' oligonucleotides with human telomeric sequence in the presence of Na<sup>+</sup> ions has an antiparallel structure with a basket strand orientation. The CD positive band at 297 nm is due to G-G base stacking (Kypr et al. 2009; Wei et al. 2008).

The CD spectrum of the 20  $\mu$ M of the antiparallel G-quadruplex 5'-AG<sub>3</sub>(T<sub>2</sub>AG<sub>3</sub>)<sub>3</sub>-3' was monitored as it was titrated with increasing concentration of the [Zn(3-Me-pic)<sub>2</sub>(phen)] complex (from 60 to 120  $\mu$ M). The intensity of both the positive band at 296 nm and the negative band at 267 nm of the CD spectrum is enhanced by the addition of the zinc complex (Fig. 5, spectrum II). The enhancement of the positive band at 296 nm due to G-G base stacking suggests partial intercalation between G-tetrads by the zinc complex, reminiscence of enhancement of positive, base-base stacking band at  $\sim$ 270 nm attributed to intercalation of B-form duplex DNA by metallointercalators. The enhancement of the positive band at 295 nm of the G-quadruplex CD spectrum by the zinc complex is the opposite to that observed for the interaction of acridine and bis-acridine with G-quadruplex where the decrease in the intensity of the positive band at 293 nm was interpreted as destabilization of the quadruplex structure (Nagesh and Krishnaiah 2003). Thus, enhancement of the positive band of the CD spectrum of the present quadruplex suggests stabilization of the antiparallel quadruplex structure by the zinc complex. When the mole ratio of the



quadruplex:zinc complex increases from 1:3 to 1:4, an induced positive band at 279 nm is completely formed (Fig. 5, spectrum III). This intense induced positive band is similar to those which resulted from zinc complex binding to the B-form duplexes used in this study (Figs. 2, 3, 5b). We are, as yet, unable to interpret the formation of this induced band. Except for this induced band, the overall shape of G-quadruplex remains unchanged, suggesting retention of the anti-parallel structure. In contrast, CD spectral titration of ruthenium(II) complexes with known intercalating ligands, viz.  $[\text{Ru}(\text{phen})_2(\text{dpqC})]^{2+}$ ,  $[\text{Ru}(\text{phen})_2(\text{dpq})]^{2+}$ ,  $[\text{Ru}(\text{phen})_2(\text{dppz})]^{2+}$  and  $[\text{Ru}(\text{phen})_3]^{2+}$ , with four stranded G-quadruplex (TTGGGGGT)<sub>4</sub> shows significant decrease in ellipticity of both CD positive and negative bands with increasing Ru(II)-complex: G-quadruplex ratio (Talib et al. 2008). The positive CD band at 265 nm was found to be split into two distinct bands at higher concentration of Ru(II)-complex. In contrast, the positive band at 296 nm of the CD spectrum of the single strand G-quadruplex 5'-AG<sub>3</sub> (T<sub>2</sub>AG<sub>3</sub>)<sub>3</sub>-3' seems to be split into two distinct bands with higher  $[\text{Zn}(3\text{-Me-pic})_2(\text{phen})]$ :G-quadruplex ratio (Fig. 5a). Whether this higher mole ratio results in this splitting or merely in an additional induced band is merely interpretative.

A comparison of the interaction the zinc complex with the 24-nucleotide G-quadruplex with the complimentary 17-bp duplex by means of CD spectroscopy was undertaken. The annealed duplex has a B-form conformation as confirmed by the presence of a positive band at 279 nm due to base-stacking interaction and a negative band at 249 nm due to DNA helicity. Incubating this duplex (20  $\mu\text{M}$ ) with the zinc complex (120  $\mu\text{M}$ ) greatly enhances the positive band at 279 nm without any shift in wavelength, indicating intercalation mode of binding by the zinc complex. The negative band intensity at 249 nm becomes more enhanced and there is a red shift of this band from 249 to 253 nm. Additionally, an induced positive band at 239 nm is formed.

### Nucleolytic property

Zinc(II) is a non-redox active transition metal cation. Although many mononuclear and multinuclear zinc(II) complexes can bind to DNA and induce

hydrolytic cleavage of DNA or model substrate, some are inactive because of the requirement of coordination unsaturation and presence of labile bonded nucleophile or nucleophilic pendant (Liu et al. 2004; Mancin and Tecilla 2007; He et al. 2009). In this study, we examine the ability of co-ordinately saturated  $[\text{Zn}]$

$(3\text{-Me-pic})_2(\text{phen})]$  to cleave pBR322 under hydrolytic conditions and in the presence of exogenous agents, sodium ascorbate (NaAsc) and hydrogen peroxide ( $\text{H}_2\text{O}_2$ ), using gel electrophoresis. Incubating the  $[\text{Zn}(3\text{-Me-pic})_2(\text{phen})]$  with pBR322 at varying concentrations of the zinc complex (10–1,000  $\mu\text{M}$ ) for 24 h at 37°C, no DNA cleavage was observed (Fig. 6). When the DNA was incubated with 30  $\mu\text{M}$  NaAsc or 30  $\mu\text{M}$   $\text{H}_2\text{O}_2$ , there is no DNA cleavage as the gel pattern is the same as that for DNA alone (Fig. 7, lanes L1–L3). Similarly, there was no significant DNA cleavage observed when the DNA was incubated with 50  $\mu\text{M}$   $\text{ZnCl}_2$  or 50  $\mu\text{M}$  zinc complex (Fig. 7, lanes L6–L7). However, when the DNA was incubated with 50  $\mu\text{M}$   $\text{ZnCl}_2$  or 50  $\mu\text{M}$  zinc complex in the presence of 30  $\mu\text{M}$  NaAsc or 30  $\mu\text{M}$   $\text{H}_2\text{O}_2$ , there was noticeable increase in the intensity of the nicked band. The activation of zinc complex towards single strand DNA cleavage by sodium ascorbate is greater than that for the  $\text{ZnCl}_2$ , suggesting coordination of the ligands results in slight increase in nucleolytic efficiency of the zinc(II) ion. Nucleolytic activation of  $[\text{Zn}(3\text{-Me-pic})_2(\text{phen})]$  by ascorbate is greater than that by  $\text{H}_2\text{O}_2$  as evidenced by the thicker nicked band (Fig. 7, L10 & L13). A previous study reported that 100  $\mu\text{M}$  of two zinc(II) complexes containing modified bipyridyl ligand with

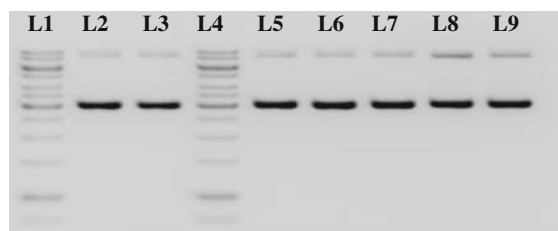


**Fig. 6** Electrophoresis results of incubating pBR322 (0.5  $\mu\text{g}/\mu\text{l}$ ) in the presence of  $[\text{Zn}(3\text{-Me-pic})_2(\text{phen})]$  in TN buffer (5 mM Tris, 50 mM NaCl) pH 7.5 at 37°C for 24 h. L1 & L4, gene ruler 1 Kb DNA ladder; L2, DNA alone; L3, DNA + 1,000  $\mu\text{M}$   $\text{ZnCl}_2$ ; DNA + various complex concentrations L5–L9: L5, 10  $\mu\text{M}$ ; L6, 50  $\mu\text{M}$ ; L7, 250  $\mu\text{M}$ ; L8, 500  $\mu\text{M}$ ; L9, 1,000  $\mu\text{M}$

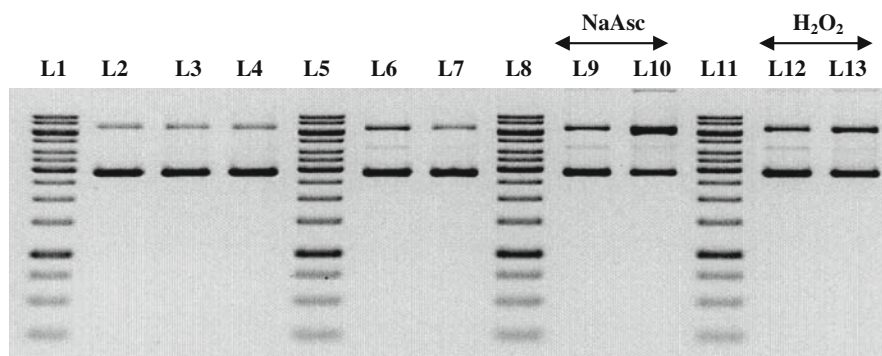


**Fig. 7** Electrophoresis results of incubating pBR322 (0.5  $\mu\text{g}/\mu\text{l}$ ) with  $\text{ZnCl}_2$  or  $[\text{Zn}(3\text{-Me-pic})_2(\text{phen})]$  in TN buffer (5 mM Tris, 50 mM NaCl) pH 7.5 at  $37^\circ\text{C}$  for 2 h in the absence and presence of exogenous agents. *L1, L5, L8, L11*: gene ruler 1 Kb DNA ladder; *L2*, DNA alone; *L3*,

DNA + 30  $\mu\text{M}$  NaAsc; *L4*, DNA + 30  $\mu\text{M}$   $\text{H}_2\text{O}_2$ ; *L6*, DNA + 50  $\mu\text{M}$   $\text{ZnCl}_2$ ; *L7*, DNA + 50  $\mu\text{M}$  Zn complex. Lanes 9–10 DNA + 50  $\mu\text{M}$  compound + 30  $\mu\text{M}$  NaAsc: *L9*,  $\text{ZnCl}_2$ ; *L10*, Zn complex. Lanes 12–13 DNA + 50  $\mu\text{M}$  compound + 30  $\mu\text{M}$   $\text{H}_2\text{O}_2$ : *L12*,  $\text{ZnCl}_2$ ; *L13*, Zn complex

guanidinium groups cannot cleave pBR322 but can do so efficiently in the presence of 0.10 mM  $\text{H}_2\text{O}_2$  (He et al. 2009). Similar activation of some zinc(II) of 1,4,7,10-tetraazacyclododecane ligand with an imidazolium side chain by ascorbate has been reported (Li et al. 2006). To investigate further the role of ascorbate and  $\text{H}_2\text{O}_2$  in activating the  $[\text{Zn}(3\text{-Me-pic})_2(\text{phen})]$ , free radical scavengers, viz. sodium azide (singlet oxygen radical scavenger), tiron (superoxide anion radical scavenger) and thiourea (hydroxyl radical scavenger), were used. DNA nicking by the zinc complex in the presence of ascorbate was not inhibited by these scavengers while that in the presence of  $\text{H}_2\text{O}_2$  could only be inhibited by thiourea (data not shown). Thus, DNA cleavage by the zinc complex in the presence of  $\text{H}_2\text{O}_2$  involves  $\cdot\text{OH}$  radical as active species and the catalytic role of the zinc complex is indicated. The cleavage mechanism involving activating the zinc complex by the ascorbate is as yet unknown and unreported.

### Topo I inhibition

DNA topoisomerases are proteins that solve topological problems accompanying key nuclear processes such as DNA replication, transcription, repair, and chromatin assembly by introducing temporary single- or double-strand breaks in the DNA (Carey et al. 2003). Topoisomerase I (topo I) manipulate coiling by unwinding duplex DNA, resulting in a more relaxed structure. It binds to the duplex DNA, cleaves a phosphodiester bond of one strand, passes the other strand through the nick and then relegates the nick. Human topo I can relax both positive and negative supercoils.

Supercoiled plasmid DNA pBR322 is suitable substrate for study with topoisomerase I, which is one strand DNA cutter. The supercoiled pBR322 (Form I) is very compact and moves faster in the gel during electrophoresis. When one strand of the supercoiled DNA is cut, the resultant unwinded, more relaxed

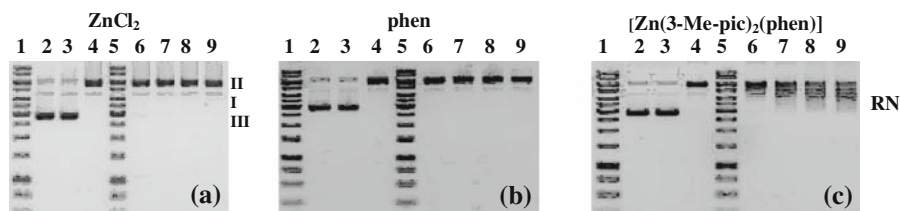


**Fig. 8** Human topoisomerase I inhibition assay by gel electrophoresis. Electrophoresis results of incubating human topoisomerase I (1 unit/21  $\mu\text{l}$ ) with pBR322 in the absence or presence of varying concentration of **a**  $\text{ZnCl}_2$ , **b** phen, **c**  $[\text{Zn}(3\text{-Me-pic})_2(\text{phen})]$ . *L1, L5*: 1 kb DNA ladder; *L2*, plasmid

pBR322; *L3*, DNA + 40  $\mu\text{M}$  compound; *L4*, DNA + 1 unit topo I. Lanes 6–9 DNA + 1 unit topo I + varying concentration of compound: *L6*, 5  $\mu\text{M}$ ; *L7*, 10  $\mu\text{M}$ ; *L8*, 20  $\mu\text{M}$ ; *L9*, 40  $\mu\text{M}$

open circular pBR322 (Form II) is formed and this nicked DNA moves slower. When two strands of the supercoiled DNA are cut, the linear DNA (Form III) is formed and it moves at intermediate speed. The commercial pBR322 (4.4 kb) has a small amount of both more relaxed Form II and Form III DNA (Fig. 8a–c: lanes 1). Under electrophoresis conditions it was possible to fully separate nicked plasmid pGEM-9Zf(–) (2.9 kb) (uppermost band, labeled Form II) from topoisomers that are relaxed to different degrees by topo I (intermediate bands, labeled ‘RN’) (Webb and Ebeler 2008). In our DNA relaxation assay, one unit of human topo I can completely convert all the supercoiled plasmid pBR322 (4.4 kb) to fully relaxed topoisomer, which is the completely unwound covalently bonded closed circular DNA (Fig. 8, lane 4). This is found in the slowest moving DNA band (labelled Form II) which contains the fully relaxed closed circular pBR322 and the originally present, small amount of nicked DNA (Diana et al. 2008). The difference in plasmid size (compared with the one used by Webb) may account for the inability to separate the fully relaxed pBR322 from the nicked pBR322. Incubating the pBR322 with the highest concentration of test compound ( $\text{ZnCl}_2$ , phen, zinc complex) from 4 to 40  $\mu\text{M}$ , no cleavage or unwinding of the DNA was observed as the banding pattern is the same as the control without any added test compound (Fig. 8, lane 3). As can be seen from Fig. 8a and b (lanes 6–9), the  $\text{ZnCl}_2$  and phen do not inhibit the activity of the topo I as the DNA bands are the same as those observed for DNA incubated with topo I alone. The present negative results for the  $\text{ZnCl}_2$  is in agreement with previous findings which found that its concentration needed to be above 80  $\mu\text{M}$  to significantly inhibit topo I and presence of high excess of  $\text{MgCl}_2$  was needed (Douvas et al. 1991). Very high concentration of  $\text{ZnCl}_2$  (mM levels) was also reportedly needed to inhibit topo I isolated from shrimp *Penaeus japonicus* (Chuang et al. 1996). However, incubating the pBR322 with human topo I and increasing concentration of the  $[\text{Zn}(3\text{-Me-pic})_2(\text{phen})]$  complex gives rise to reduction of the nicked band (containing nicked and fully relaxed DNA) and formation of various faster moving bands of topoisomers with different degree of relaxation (RN). At 10  $\mu\text{M}$  of the zinc complex, unchanged supercoiled DNA band starts to appear (Fig. 8c, lane 7). The appearance of

slower moving bands of less relaxed topoisomers is observed with increasing concentration of the zinc complex (Fig. 8c, lanes 6–9). These results show that the zinc complex can inhibit the function of topo I in relaxing the supercoiled pBR322, and also show that the degree of inhibition is concentration dependent. This zinc complex is a topo I inhibitor and not a topo I poison (which prevents the nicked DNA from relegation).

As a preliminary investigation into the mechanism of action of the above topo I inhibition, we used three variations of mixing the DNA, topo I and the zinc complex (at 50  $\mu\text{M}$ ) for the topo I inhibition assay. When the three components are mixed simultaneously, there is extensive inhibition as a fastest wide band appears and this consists of supercoiled DNA and poorly relaxed DNA (Fig. 9, lane 5). The light bands of topoisomers with different degree of relaxation can be seen. When the DNA is first incubated with zinc complex for 30 min before adding the topo I, the fastest moving band is wider, thereby appearing to be nearer to the slowest moving band (Form II). Incubating the topo I with zinc complex first before adding the DNA results in the fastest moving band (Fig. 9, lane 7) which is widest and which is positioned intermediate between those in lane 5 and lane 8. These observed differences in inhibition of topo I suggest initial binding of the zinc complex to either the topo

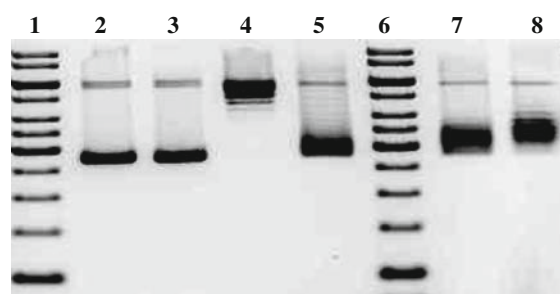


**Fig. 9** Effect of sequence of mixing for the human topoisomerase I inhibition assay. Electrophoresis results of incubating human topoisomerase I (1 unit/21  $\mu\text{l}$ ) with pBR322 (0.5  $\mu\text{g}/\mu\text{l}$ ) and 50  $\mu\text{M}$   $\text{Zn}(3\text{-Me-pic})_2(\text{phen})$ . Lanes 1 & 6: 1 kb DNA ladder; L2: DNA alone; L3: DNA + zinc complex alone; L4: DNA + 1 unit topo I; L5: simultaneous mixing DNA + topo I + zinc complex; L7: incubated topo I + zinc complex for 30 min, then added DNA with further incubation for another 30 min; L8: incubated DNA + zinc complex for 30 min, then added topo I and further incubation for another 30 min

I or the DNA give rise to differences in mode of action. Further investigation is underway. In addition, it is noted that 50  $\mu\text{M}$  this zinc complex is highly efficient topo I inhibitor compared to  $\text{ZnCl}_2$  which was reported to inhibit less than 10% of topo I activity at 50  $\mu\text{M}$  and which could totally inhibit topo I at 300  $\mu\text{M}$  (Douvas et al. 1991).

## Conclusion

The  $[\text{Zn}(\text{3-Me-pic})_2(\text{phen})]$  complex shows nucleobase sequence binding selectivity with the following order: ATAT > AATT > CG. We postulate that the nature of the 3-methyl-picolinate ligand (as hydrogen bonding capability and  $\text{C-H}\cdots\pi$ ) and the relative orientation of picolinate ligands with respect to the phen ligand predisposes the zinc complex towards the observed DNA recognition. Intercalation of the phen moiety between diagonal nucleobases on opposite DNA strands or adjacent bases on the same DNA strand fixed the orientation of the chelated 3-methylpicolinate ligands for favourable or less favourable interaction with the type of adjacent nucleobases. Besides this DNA binding selectivity, the zinc complex appears to stabilize the G-quadruplex. It can also efficiently inhibit the function of topo I. These two latter properties indicate the potential of this zinc complex as a new targeting anticancer drug. Preliminary investigation shows that it is antiproliferative against MCF-7 breast cancer cells with an  $\text{IC}_{50}$  value of 4.8  $\mu\text{M}$  for 72 h incubation (S. T. Von and C. H. Ng (2009) unpublished data).

## Supplementary data

Supplementary data associated with this article can be found in the online version. CCDC No. 731838 contains the supplementary crystallographic data for this paper. It can be obtained free of charge from The Cambridge Crystallographic Data Centre via [www.ccdc.cam.ac.uk/data\\_request/cif](http://www.ccdc.cam.ac.uk/data_request/cif).

**Acknowledgments** The authors like to thank MOSTI of Malaysia for an Science grant (02-02-11-SF0033). IC thanks CNPq (Proc. 472237/2008-0) and Fundunesp (Proc. 00525/08-DFP).

## References

- Address KJ, Sinsheimer JS, Feigon J (1993) Solution structure of a complex between [N-MeCys3, N-MeCys7]TANDEM and [d(GATATC)]<sub>2</sub>. *Biochemistry* 32:2498–2508
- Baker ES, Bernstein SL, Gabelica V, De Pauw E, Bowers MT (2006) G-quadruplexes in telomeric repeats are conserved in a solvent-free environment. *Int J Mass Spectrom* 253: 225–237
- Bazzicalupi C, Bencini A, Bonaccini C, Giorgi C, Gratterer P, Moro S, Palumbo A, Simionato A, Sgrignani J, Sissi C, Valtancoli B (2008) Tuning the activity of Zn(II) complexes in DNA cleavage: clues for design of new efficient metallo-hydrolases. *Inorg Chem* 47:5473–5484
- Beretta GL, Perego P, Zunino F (2008) Targeting topoisomerase I: molecular mechanisms and cellular determinants of response to topoisomerase I inhibitors. *Expert Opin Ther Targets* 12:1243–1256
- Boger DL, Fink BE, Brunette SR, Tse WC, Hedrick MP (2001) A simple, high-resolution method for establishing DNA binding affinity and sequence selectivity. *J Am Chem Soc* 123:5878–5891
- Boseggia E, Gatos M, Lucatello L, Mancin F, Moro S, Palumbo M, Sissi C, Tecilla P, Tonellato U, Zagotto G (2004) Toward efficient Zn(II)-based artificial nucleases. *J Am Chem Soc* 126:4543–4549
- Bruker (2007) APEX2 and SAINT. Bruker AXS Inc, Madison
- Carey JF, Schultz SJ, Sisson L, Fazzio TG, Champoux JJ (2003) DNA relaxation by human topoisomerase I occurs in the closed clamp conformation of the protein. *Proc Nat Acad Sci* 100:5640–5645
- Chuang N-N, Lin C-L, Chen H-K (1996) Modification of DNA topoisomerase I enzymatic activity with phosphotyrosyl protein phosphatase and alkaline phosphatase from the hepatopancreas of the shrimp *Penaeus japonicus* (Crustacea: Decapoda). *Comp Biochem Physiol* 114B: 145–151
- Desai AN, Shankar V (2003) Single-strand-specific nucleases. *FEMS Microbiol Rev* 26:457–491
- Diana P, Martorana A, Barraja P, Montalbano A, Dattolo G, Cirrincione G, Dall'Acqua F, Salvador A, Vedaldi D, Basso Giuseppe, Viola G (2008) Isoindolo[2,1-a]quinoxaline derivatives, novel potent antitumour agents with dual inhibition of tubulin polymerization and topoisomerase I. *J Med Chem* 51:2387–2399
- Di Marco VB, Tapparo A, Dolmella A, Bombi GG (2004) Complexation of 2-hydroxynicotinic and 3-hydroxypicolinic acids with zinc(II). Solution state study and crystal structure of *trans*-diaqua-bis-(3-hydroxypicolinato)zinc(II). *Inorg Chim Acta* 357:135–142
- Douvas A, Lambie PB, Turman MA, Nitahara KS, Hammond L (1991) Negative regulation of Sc1-70/topoisomerase I by zinc and an endogenous macromolecule. *Biochem Biophys Res Commun* 178:414–421
- DS VISUALIZER™—Accelrys Software Inc. Discovery Studio Visualizer 2.0
- Galezowska E, Masternak A, Rubis B, Czyrski A, Rybzyńska, Hermann TW, Juskowia B (2007) Spectroscopic study and G-quadruplex DNA binding affinity of two

- bioactive papaverine-derived ligands. *Int J Biol Macro* 41: 558–563
- He J, Sun J, Mao Z-W, Ji L-N, Sun H (2009) Phosphodiester hydrolysis and specific DNA binding and cleavage promoted by guanidinium-functionalized zinc complexes. *J Inorg Biochem* 103:851–858
- Ivanow VI, Minchenkova LE, Schyolkina AK, Poletayer AI (1973) Different conformations of double-stranded nucleic acid in solution as revealed by circular dichroism. *Biopolymers* 12:89–110
- Jiang A-L, Cheng Y, Li J, Zhang W (2008) A zinc-dependent endonuclease is responsible for DNA laddering during nuclear salt-induced programmed cell death in root tip cells of rice. *J Plant Physiol* 165:1134–1141
- Jones G, Willet P, Glen RC (1995) Molecular recognition of receptor sites using a genetic algorithm with a description of desolvation. *J Mol Biol* 245:43–53
- Jones G, Willet P, Glen RC, Leach AR, Taylor R (1997) Development and validation of a genetic algorithm for flexible docking. *J Mol Biol* 267:727–748
- Kikuta E, Koike T, Kimura E (2000) Controlling gene expression by zinc(II)–macrocyclic tetraamine complexes. *J Inorg Biochem* 79:253–259
- Kumar Singh S, Joshi S, Ranjan Singh A, Saxena JK, Pandey DS (2007) DNA binding and topoisomerase II inhibitory activity of water-soluble ruthenium(II) and rhodium(III) complexes. *Inorg Chem* 46:10869–10876
- Kypř J, Kejnovská I, Renčičuk D, Vorličková M (2009) Circular dichroism and conformational polymorphism of DNA. *Nucleic Acids Res* 37:1713–1725
- Li Q-L, Huang J, Wang Q, Jiang N, Xia C-Q, Lin H-H, Wu J, Yu X-Q (2006) Monometallic complexes of 1, 4, 7, 10-tetraazacyclododecane containing an imidazolium side: synthesis, characterization, and their interaction with plasmid DNA. *Bioorg Med Chem* 14:4151–4157
- Li J-H, Wang J-T, Zhang L-Y, Chen Z-N, Mao Z-W (2009) Structure, speciation, DNA binding and nuclease activity of two bipyridyl-zinc complexes bearing trimethylammonium groups. *Inorg Chim Acta* 362:1918–1924
- Lin L, Ozaki T, Takada Y, Kageyama H, Nakamura Y, Hata A, Zhang J-H, Simonds WF, Nakagawara A, Koseki H (2005) Topors, a p53 and topoisomerase I-binding RING finger protein, is a coactivator of p53 in growth suppression induced by DNA damage. *Oncogene* 24:3385–3396
- Liu C-L, Wang M, Zhang T-L, Sun H-Z (2004) DNA hydrolysis promoted by di- and multi-nuclear metal complexes. *Coord Chem Rev* 248:147–168
- Lu Y-J, Ou T-M, Tan J-H, Hou J-Q, Shao W-Y, Peng D, Sun N, Wang X-D, Wu W-B, Bu X-Z, Huang Z-S, Ma D-L, Wong K-Y, Gu L-Q (2008) 5-N-methylated quinoline derivatives as telomeric G-quadruplex stabilising ligands: effects of 5-N positive charge on quadruplex binding affinity and cell proliferation. *J Med Chem* 51:6381–6392
- Malinina L, Soler-López M, Aymamí J, Subirana JA (2002) Intercalation of an acridine-peptide drug in an AA/TT base step in the crystal structure of [d(CGCGAATT CGCG)](2) with six duplexes and seven Mg(2+) ions in the asymmetric unit. *Biochemistry* 41:9341–9348
- Mancin F, Tecilla P (2007) Zinc(II) complexes as hydrolytic catalysts of phosphate diester cleavage: from model substrates to nucleic acids. *New J Chem* 31:800–817
- Nagaoka M, Sugiura Y (2000) Artificial zinc finger peptides: creation, DNA recognition, and gene regulation. *J Inorg Biochem* 82:57–63
- Nagesh N, Krishnaiah A (2003) A comparative study on the interaction of acridine and synthetic bis-acridine with G-quadruplex structure. *J Biochem Biophys Methods* 57: 65–74
- Ng CH, Kong KC, Von ST, Balraj P, Jensen P, Thirthagiri E, Hamad H, Chikira M (2008) Synthesis, characterization, DNA-binding study and anticancer property of ternary metal(II) complexes of EDDA and an intercalating ligand. *Dalton Trans* (4):447–454
- Nordell P, Westerlund F, Wilhelmsson M, Nordén B, Lincoln P (2007) Kinetic recognition of AT-rich DNA by ruthenium complexes. *Angew Chem Int Ed* 46:2203–2206. Also references quoted therein
- Okabe N, Oya N (2000) Copper(II) and zinc(II) complexes of pyridine-2, 6-dicarboxylic acid. *Acta Crystallogr C* 56: 305–307
- Papworth M, Kolasinska P, Minczuk M (2006) Designer zinc-finger proteins and their applications. *Gene* 366:27–38
- Patra AK, Bhowmick T, Ramakumar S, Chakravarty AR (2007) Metal-based netropsin mimics showing AT-selective DNA binding and DNA cleavage activity at red light. *Inorg Chem* 46:9030–9032
- Pedretti A, Villa L, Vistoli G (2002) Vega: a versatile program to convert, handle and visualize molecular structure on windows-based PCs. *J Mol Graph* 21:47–49
- Pedretti A, Villa L, Vistoli G (2003) Atom-type description language: a universal language to recognize atom types implemented in the vega program. *Theor Chem Acta* 109:229–232
- Pedretti A, Villa L, Vistoli G (2004) Vega—an open platform to develop chemo-bio-informatics applications, using plug-in architecture and script programming. *J Comput Aided Mol Des* 18:167–173
- Pommier Y (2008) Topoisomerase I inhibitors: camptothecins and beyond. *Nat Rev Cancer* 6:789–802
- Proudfoot EM, Mackay JP, Vagg RS, Vickery KA, Williams PA, Karuso P (1997) D-*cis*- $\alpha$ -[Ru(RR-picchnMe<sub>2</sub>)(phen)]<sup>2+</sup> shows minor groove AT selectivity with oligonucleotides. *Chem Comm* (17):1623–1624
- Qian J, Gu W, Liu H, Gao F, Feng L, Yan S, Liao D, Cheng P (2007) The first dinuclear copper(II) and zinc(II) complexes containing novel bis-TACN: syntheses, structures, and DNA cleavage activities. *Dalton Trans* (10):1060–1066
- Rajendiran V, Murali M, Suresh E, Palaniandavar M, Periasamy VS, Akbarsha MA (2008) Non-covalent DNA binding and cytotoxicity of certain mixed-ligand ruthenium(II) complexes of 2,2'-dipyridylamine and diimines. *Dalton Trans* (16):2157–2170
- Rajendran A, Nair BU (2006) Unprecedented binding behaviour of acridine group of dye: a combined experimental and theoretical investigation for the development of anticancer chemotherapeutic agents. *Biochim Biophys Acta* (1760):1794–1801
- Ramakrishnan S, Palaniandavar M (2008) Interaction of *rac*-[Cu(diimine)<sub>3</sub>]<sup>2+</sup> and *rac*-[Zn(diimine)<sub>3</sub>]<sup>2+</sup> complexes with CT DNA: effect of fluxional Cu(II) geometry on DNA binding, ligand-promoted exciton coupling and prominent DNA cleavage. *Dalton Trans* (29):3866–3878

- Rothenberg ML (1997) Topoisomerase I inhibitors: review and update. *Ann Oncol* 8:837–855
- Seng HL, Alan Ong HK, Raja Noor ZRAR, Bohari MY, Tie-kink ERT, Tan KW, Mohd Jamil M, Caracelli I, Ng CH (2008) Factors affecting nucleolytic efficiency of some ternary metal complexes with DNA binding and recognition domains. Crystal and molecular structure of Zn(phen)(edda). *J Inorg Biochem* 102:1997–2011
- Seng HL, Tan KW, Mohd Jamil M, Tan WT, Hamada H, Chikira M, Ng CH (2009) Copper(II) complexes of methylated glycine derivatives: effect of methyl substituent on their DNA binding and nucleolytic property. *Polyhedron* 28:2219–2227
- Sheldrick GM (1996) SADABS. University of Göttingen, Germany
- Sheldrick GM (2008) A short history of SHELX. *Acta Crystallogr A* 64:112–122
- Stehbens WE (2003) Oxidative stress, toxic hepatitis, and antioxidants with particular emphasis on zinc. *Exp Mol Pathol* 75:265–276
- Sunami S, Nishimura T, Nishimura I, Ito S, Arakawa H, Ohkubo M (2009) Synthesis and biological activities of topoisomerase I inhibitors, 6-arylmethylamino analogues of edotecarin. *J Med Chem* 52:3225–3237
- Talib J, Green C, Davis KJ, Urathamakul T, Beck JL, Aldrich-Wright JR, Ralph SF (2008) A comparison of the binding of metal complexes to duplex and quadruplex DNA. *Dalton Trans* 1018–1026
- Teicher BA (2008) Next generation topoisomerase I inhibitors: rationale and biomarker strategies. *Biochem Pharmacol* 75:1262–1271
- Wang X, Wang L-K, Kingsbury WD, Johnson RK, Hecht SM (1998) Differential effects of camptothecin derivatives on topoisomerase I-mediated DNA structure modifications. *Biochemistry* 37:9399–9408
- Wang Y, Schnetz-Boutaud NC, Kroth H, Yagi H, Sayer JM, Kumar S, Jerina DM, Stone MP (2008) 3'-Intercalation of a N2-dG 1R-*trans*-anti-benzo[c]phenanthrene DNA adduct in an iterated (CG)<sub>3</sub> repeat. *Chem Res Toxicol* 21:1348–1358
- Waterborg JH, Kuyper CMA (1982) Substrate specificity and mode of action of the zinc-metallo nuclease from *Physarum polycephalum*. *J Biochem* 92:1655–1661
- Webb MR, Ebeler SE (2008) Comparative analysis of topoisomerase IB inhibition and DNA intercalation by flavonoids and similar compounds: structural determinates of activity. *J Food Biochem* 32:576–596
- Wei C, Tang Q, Li C (2008) Structural transition from the random coil to quadruplex of AG<sub>3</sub>(T<sub>2</sub>AG<sub>3</sub>)<sub>3</sub> induced by Zn<sup>2+</sup>. *Biophys Chem* 132:110–113
- Xu Y, Noguchi Y, Sugiyama H (2006) The new models of the human telomere d[AGGG(TTAGGG)<sub>3</sub>] in K<sup>+</sup> solution. *Bioorg Med Chem* 14:5584–5591
- Zeglis BM, Pierre VC, Barton JK (2007) Metallo-intercalators and metallo-insertors. *Chem Commun* (45):4565–4579
- Zhang N, Lin C, Huang X, Kolbanovskiy A, Hingerty BE, Amin S, Broyde S, Geacintov NE, Patel DJ (2005) Methylation of cytosine at C5 in a CpG sequence context causes a conformational switch of a benzo[a]pyrene diol epoxide-N2-guanine adduct in DNA from a minor groove alignment to intercalation with base displacement. *J Mol Biol* 346:951–965
- Zhang W-J, Ou T-M, Lu Y-J, Huang Y-Y, Wu W-B, Huang Z-S, Zhou J-L, Wong K-Y, Gu L-Q (2007) 9-Substituted derivatives as G-quadruplex stabilising ligands in telomeric DNA. *Bioorg Med Chem* 15:5493–5501